

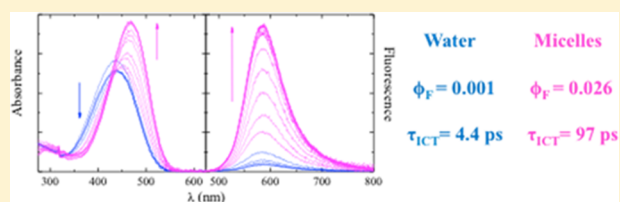
Inclusion of Two Push–Pull *N*-Methylpyridinium Salts in Anionic Surfactant Solutions: A Comprehensive Photophysical Investigation

Alessio Cesaretti,^{*,†} Benedetta Carlotti,[†] Giuseppe Consiglio,[‡] Tiziana Del Giacco,[†] Anna Spalletti,[†] and Fausto Elisei[†]

[†]Department of Chemistry, Biology and Biotechnology and Centro di Eccellenza sui Materiali Innovativi Nanostrutturati (CEMIN), University of Perugia, Perugia, Italy

[‡]Department of Industrial Engineering, University of Catania, viale Andrea Doria 6, I-95125 Catania, Italy

ABSTRACT: Two *N*-methylpyridinium salts with push–pull properties have been investigated in the aqueous solution of anionic micelles of sodium dodecyl sulfate (SDS) and potassium *p*-(octyloxy)benzenesulfonate (*p*OoBSK) surfactants. These molecules are known to be extremely sensitive to the local environment, with their absorption spectrum being subjected to a net negative solvatochromism. These compounds are also characterized by an excited state deactivation strictly dependent on the physical properties of the chemical surrounding, with the formation of intramolecular charge-transfer (ICT) states accordingly stabilized. Thanks to steady-state and femtosecond resolved spectroscopic techniques, the photophysical properties of these molecules in the presence of anionic micelles have been fully characterized and an efficient permeation within the micellar aggregates can thus be inferred. The extent of the changes in the photophysical properties of these molecules (with respect to what is observed in water) is an indicator of the medium experienced in the nanoheterogeneous solutions: enhanced fluorescence emissions, reduced Stokes shifts and slowed-down excited state decays strongly confirm the confinement within a scarcely polar and restraining environment. The slightly different behavior shown in the two types of micelles can be ascribed to a peculiar interaction between the aromatic moiety of the surfactant and that of the cations. Additionally, the inclusion promotes the solubilization of these poorly water-soluble salts, which is alluring in their promising use as DNA binders for antitumor purposes. Thus, the anionic micelles allowed the solubilization of the pyridinium salts under investigation, which in turn allowed the characterization of the nonhomogeneous medium established by the micellar aggregates.



INTRODUCTION

Stilbene-like compounds bearing electron donor/acceptor (D/A) units are of the utmost interest because of their multipurpose applications.^{1–10} A long-term project of our group has been indeed devoted to quaternized azastilbene molecules with push–pull nature, where the acceptor character is bestowed upon one moiety of the molecule by the methylpyridinium unit and specific substituents on the other end bring electron donor properties.^{11–14} These *push–pull* compounds could be exploited as optoelectronics/photonics materials for their nonlinear optical (NLO) properties¹⁵ and as anticancer drugs for their ability to form complexes with DNA.¹⁶ This latter feature has been the object of a number of works, where *N*-methylpyridinium salts and analogous compounds were found to bind the DNA macromolecule.^{17–21}

This finding is extremely promising in light of a potential antitumor activity performed by these compounds, but the sparing water solubility of these molecules is an issue to be reckoned with, which might be overcome by means of surfactant or polymeric micelle vehicles.^{22–24}

Micelles, being *de facto* nearly spherical surfactant aggregates formed in aqueous solution, are indeed extremely appealing systems for their ability to swallow molecules within their structure, providing a useful tool for the dissolution of poorly

water-soluble molecules. This ability is essential when dealing with compounds of potential pharmacological interest. Micellar aggregates have therefore been largely employed as drug vehicles, for they make the drugs ready for use and help controlling their trajectory in the human body for a targeted drug delivery.^{25–30}

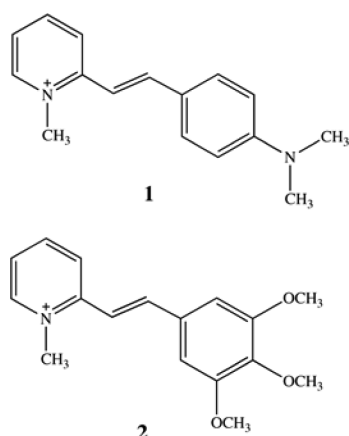
Moreover, the effect of the polarity and viscosity of the solvent on the spectral and photophysical properties of pyridinium salts has been broadly investigated. Many groups have studied the major influence of the environment on the steady state and dynamic properties of these molecules, both in homogeneous and microheterogeneous media.^{31–35} Particularly, our group has focused its attention on some molecules belonging to this family, namely, the *trans* isomers of the 2-*D*-vinyl-1-methylpyridinium cation, where *D* represents an electron donor group, which is the 4-dimethylaminophenyl (1) and 3,4,5-trimethoxyphenyl (2), respectively (Scheme 1).^{36,37} A substantial negative solvatochromism has been found in the absorption spectrum of these molecules, whereas

Received: March 10, 2015

Revised: April 30, 2015

Published: May 6, 2015

Scheme 1. Molecular Structures of the *trans* (E) Isomers of the Iodides of 2-D-Ethenyl-1-methylpyridinium^a



^aD = 4-(dimethylamino)phenyl (1) and 3,4,5-trimethoxyphenyl (2).

their emission is affected to a minor degree by the solvent polarity.³⁶

These spectral features have been explained by taking into account the different nature of the electronic states presumably involved in the absorption and emission processes, whose character has also been suggested by quantum-mechanical calculations.^{36,38} The ground state is defined by a large dipole moment, owing to the positive charge localized on the strong electron-withdrawing cationic pyridinium ring, while the excited Franck–Condon state shows a much lower dipole moment, because of a charge migration from the D to the A unit. A third state is involved in the deactivation of these molecules in what is an intramolecular charge transfer (ICT) state, where the charge moves back from A to D, thus enhancing the charge separation and the dipole moment of the excited ICT state. Its dipole moment resembling that of the polar ground state justifies the invariance of the fluorescence band energy irrespective of solvent polarity, even though its molecular structure has ignited ongoing controversy. In solvents with high polarity and in the presence of suitable D substituents, the formation of this state is thought to come with the twisting of the *N*-methylpyridinium group around the quasi-single bond with the ethene bridge (TICT).³⁶ When a TICT state is formed, the back-charge transfer is extremely efficient and the internal conversion becomes the main deactivation channel for this excited state. Depending on the efficiency of the D unit, its hindrance and solvent physical properties, the relative level of stability between ground and excited states and also between the locally excited (LE) and ICT states can therefore be considerably altered; additionally, utterly different spectral photophysical and kinetic properties can be retrieved. The Stokes shift experiences a drastic increase in highly polar solvents where the polar ground state gets stabilized moving the absorption spectrum to higher energies; the fluorescence quantum yield is enhanced by up to 2 orders of magnitude, as a result of increased viscosity and/or reduced polarity which limit the ICT process; the singlet excited state dynamics is greatly affected, with lifetimes ranging from a few picoseconds in water for those molecules allowing an efficient charge separation via plausible TICT formation to hundreds of picoseconds in viscous and nonpolar media.

In that respect, the present paper is intended as a detailed photophysical study of the aforementioned molecules in the

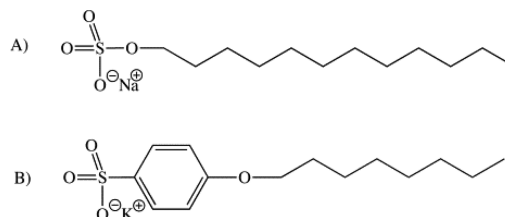
self-organized media provided by two anionic surfactants: the commercial sodium dodecyl sulfate (SDS) and the laboratory-synthesized potassium *p*-(octyloxy)benzenesulfonate (*p*OoBSK). Resorting to both conventional stationary and ultrafast time-resolved spectroscopic techniques, the investigation aims at a twofold purpose: (1) proving the inclusion of the *push–pull* pyridinium salts within the micellar aggregates and (2) taking full advantage of the sensitivity of these chemical species toward the properties of the medium in order to characterize the chemical makeup experienced by the molecule.

The study hereinafter discussed intends to describe the non-heterogeneous multicomponent system under investigation by combining the solubilizing abilities of the anionic micelles with the close dependence between the photophysical properties of pyridinium salts and the physical properties of the sensed environment. In doing so, a clear picture of the *push–pull* pyridinium salts within the solubilizing micellar carriers can thus be drawn.

MATERIALS AND METHODS

Materials. The investigated molecules are depicted in Scheme 1. They were synthesized as iodide salts for previous works,^{36,37} following a procedure which has already been described elsewhere.^{1,16} All the spectroscopic measurements were carried out on samples prepared in deionized water as solvent (ELGA grade) in the presence of two anionic surfactants: sodium dodecyl sulfate (SDS) and potassium *p*-(octyloxy)benzenesulfonate (*p*OoBSK) (Scheme 2). With the

Scheme 2. Structures of the Anionic Surfactants Used: (A) Sodium-dodecylsulfate (SDS) and (B) Potassium *p*-(Octyloxy)benzenesulfonate (*p*OoBSK)



critical micellar concentration being 8×10^{-3} and 1×10^{-3} M for SDS³⁹ and *p*OoBSK, respectively, micelle containing solutions were obtained with a surfactant concentration of 3×10^{-2} M. The SDS surfactant was purchased from Sigma-Aldrich and purified twice by crystallization from methanol–acetone mixture, while the *p*OoBSK surfactant was synthesized and purified in our laboratories according to a slightly different procedure with respect to the one previously reported in the literature.^{40–42}

The strategy we adopted, which considers the two steps of the reaction proposed by Bunton et al.⁴⁰ in reverse order, leads to the formation of potassium *p*-(octyloxy)benzenesulfonate (*p*OoBSK) avoiding the formation of other organic salts as side products, which would be otherwise difficult to remove. First, *p*-(octyloxy)benzene was prepared according to the Williamson synthesis by reacting sodium phenoxide with 1-bromooctane in ethanol to reflux for 12 h. After workup, the oil obtained was purified by reduced pressure distillation to give *p*-(octyloxy)benzene as a colorless oil. B.p.: 165–167 °C (20 mmHg); ¹H NMR (CDCl₃, 200 MHz) δ 7.26 (m, 2H), 6.89 (m, 3H), 3.94 (t, 2H), 1.77 (m, 2H), 1.43 (m, 10H), 0.87 (tr, 3H). *p*OoBSK was hence prepared from *p*-(octyloxy)benzene as follows.

Concentrated sulfuric acid (10 mL) was added dropwise to *p*-(octyloxy)benzene (10.0 g, 0.048 mol), stirred and heated to 60–65 °C in an oil bath. After the resulting mixture had been stirred for 12 h, a very viscous yellow-orange liquid was obtained, which was mixed with CCl₄ (60 mL) and cooled at 4 °C. The small liquid phase formed on the bottom was separated and CCl₄ was completely removed under a vacuum. The residue was dissolved in petroleum ether and allowed to stand at –20 °C affording to obtain *p*-(octyloxy)benzenesulfonic acid as a white crystalline solid, which was filtered and collected with a Buchner funnel. The salt (*p*OoBSK) was precipitated as a white solid by mixing a solution of *p*-(octyloxy)benzenesulfonic acid with an equimolar solution of KOH and then dissolved in hot ethanol and left to crystallize. The crystalline solid (12.5 g, 80%) was then collected by filtration under a vacuum, washed with cold ethanol and acetone, and then dried under a vacuum. M.p.: 120 °C (mesophase), 285 °C (dec); ¹H NMR (D₂O, 200 MHz) δ = 0.74 (tr, 3H), δ = 1.32 (m, 10H), δ = 1.42 (m, 2H), δ = 3.55 (t, 2H), δ = 6.55 (d, 2H), δ = 7.47 (d, 2H). cmc: 1.4×10^{-2} M at 35 °C; α = 0.33.

Photophysical Measurements. Steady-state absorption and emission spectra were recorded with a PerkinElmer Lambda 800 spectrophotometer and a Fluorolog-2 (Spex, F112AI) spectrofluorometer, respectively. The latter gives back fluorescence emission spectra taking into account both the monochromator response and the detector sensitivity. Fluorescence quantum yields (experimental error of ca. 7%) were determined from the emission spectra of samples whose absorbance at the excitation wavelength was lower than 0.1, to have a linear relation between the absorbance and the emitted intensity and avoid self-absorption effects. Tetracene (ϕ_F = 0.17 in air-equilibrated cyclohexane) and 9,10-diphenylanthracene (ϕ_F = 0.73 in air-equilibrated cyclohexane)⁴³ were used as fluorimetric standards for the determination of the fluorescence quantum yields of compounds **1** and **2**, respectively, in the micellar environment.

The experimental setup for ultrafast spectroscopic and kinetic measurements was widely described elsewhere.^{44–46} The 400 nm excitation pulses of ca. 40 fs were generated by an amplified Ti:sapphire laser system (Spectra Physics, Mountain View, CA). The transient absorption setup (Helios, Ultrafast Systems, Sarasota, FL) is characterized by a temporal resolution of ca. 150 fs and a spectral resolution of 1.5 nm. Probe pulses for optical measurements were produced by passing a small portion of the 800 nm light through an optical delay line (with a time window of 3200 ps) and focusing it into a 2 mm thick sapphire or CaF₂ window to generate a white-light continuum in the 475–800 nm or 400–625 nm range, respectively, depending on the spectral region of interest. The chirp inside the sample cell was determined by measuring the laser-induced Kerr signal of water. All the measurements were carried out under magic angle conditions, in a 2 mm cell and with an absorbance ranging from 0.3 to 1.0 at 400 nm. The samples were stirred during the measurements to prevent the interferences generated by the photoreaction of the molecules. Transient absorption data were analyzed using the Surface Explorer PRO (Ultrafast Systems)^{47,48} and Glotaran softwares.⁴⁹ The first allows to perform the singular value deconvolution of the 3D surface into principal components (spectra and kinetics) followed by global analysis (giving lifetimes with an error of \approx 10% and decay associated spectra, DAS, of the detected transients).⁵⁰ Glotaran was used to perform the target

analysis assuming successive steps in order to carry out the global fit of the acquired data and provide the species associated spectra (SAS), which allow to avoid precursor–successor dynamics of the transients interfering with the calculation of their relative spectral shapes.⁴⁹

Triplet–triplet absorption spectra and triplet lifetimes (τ_T) of the molecules under investigation in the presence of micellar aggregates were measured by a nanosecond laser flash photolysis setup previously described (Nd:YAG Continuum, Surelite II, third harmonics, λ_{exc} = 355 nm, pulse width ca. 7 ns and energy \leq 1 mJ pulse⁻¹).^{51,52} The transient spectra were obtained by monitoring the change of transient absorption over the 300–900 nm spectral range and averaging at least 10 decays at each wavelength. The setup was calibrated by an optically matched solution of benzophenone (ϕ_T = 1 and ϵ_T = 6500 M⁻¹ cm⁻¹ at the corresponding absorption maximum, λ_{max} = 520 nm) in acetonitrile.⁵³

In order to minimize the interference arising from the formation of photoproducts during the measurements, the deoxygenated solutions (\sim 25 mL) of the investigated compounds were flowed through the quartz cell using a continuous-flow system. The experimental errors were estimated to be about \pm 10% for τ_T and \pm 15% for the factor $\phi_T \times \epsilon_T$. The quenching constants of the triplets by molecular oxygen were evaluated by applying the Stern–Volmer equation to the triplet lifetime measured in deaerated and air-equilibrated solutions (oxygen concentration in water: 2.9×10^{-4} M). All the ns-transient absorption measurements were carried out at room temperature on solutions which were deaerated by bubbling pure nitrogen.

RESULTS AND DISCUSSION

Absorption and Fluorescence Properties. The absorption and fluorescence properties of the pyridinium salts were studied in deionized water (where they are known to be completely dissolved without ion-pair formation)³⁶ in the presence of anionic SDS and *p*OoBSK surfactants. An anionic sulfate head and a 12-carbon aliphatic chain characterize the former, while the latter has a shorter methylenic chain (eight carbons) bonded through an oxygen atom to an aromatic ring in the *para* position with respect to the sulfonate headgroup. Resorting to anionic surfactants was a deliberate choice in order to favor the interaction between the cationic pyridinium salts and the anionic micellar aggregates. Moreover, the synthesis of the *p*OoBSK aimed at fostering the interaction between the surfactant and the two compounds by virtue of the aromaticity featured by either molecular structures.

The absorption and emission spectra of compounds **1** and **2** in highly polar water (W) and low polar dichloromethane (DCM) and in the presence of the two different surfactants are shown in Figure 1, and their absorption and fluorescence properties are listed in Table 1. Since these molecules are sensitive to changes in both the polarity and viscosity of the medium in which they are dissolved, the position of the absorption and emission bands together with the fluorescence intensities are a clear sign of the environment experienced by the molecules.³⁶

In nonmicellar solution, compounds **1** and **2** show nonstructured bell-shaped absorption bands, which undergo a negative solvatochromism; i.e., the band shifts toward lower energies by decreasing the solvent polarity. As for the fluorescence spectra of the two molecules, the emission band shape and position remain almost insensitive to polarity,

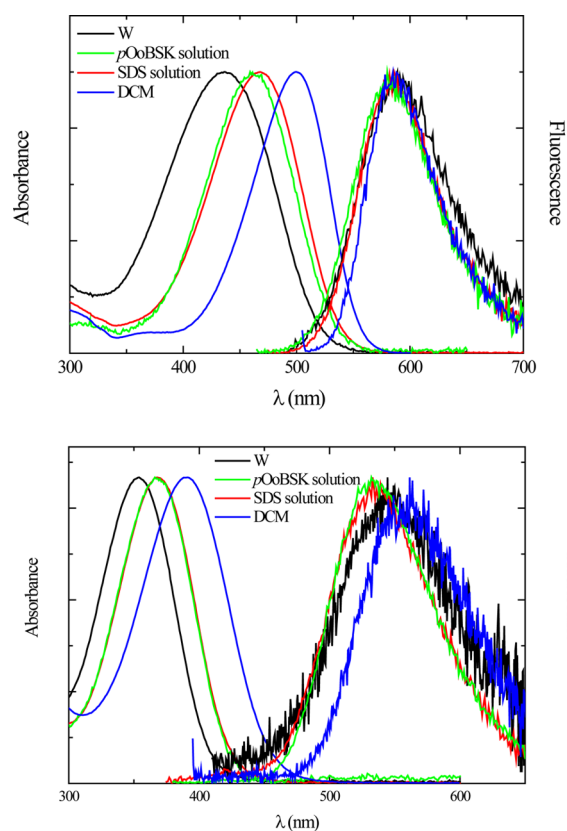


Figure 1. Normalized absorption and emission spectra of **1** (upper graph) and **2** (lower graph) in W, in DCM, and in the presence of *p*OoBSK (0.1 M) and SDS (0.1 M) solutions.

although the fluorescence quantum yield decreases by 2 orders of magnitude for compound **1** and almost 1 order of magnitude for compound **2** when going from DCM to the more polar W.

When the two compounds are dissolved in aqueous surfactant solution, significant spectral alterations are revealed: both micelles are responsible for a bathochromic shift of the absorption and a little hypsochromic shift of the emission band with respect to pure water. Interestingly, each surfactant solution induces peculiar spectral modifications for **1** and **2**: SDS micelles, probably providing a less polar environment for these compounds, cause larger shifts in the absorption spectrum; *p*OoBSK micelles are instead responsible for greater changes in the position of the emission band.

It is likely that π - π interactions among the phenyl units of the *p*OoBSK surfactant monomers define a more compact micellar aggregate, characterized either by reduced water content or more structured water, thus acting as a more viscous environment for the pyridinium salts (*vide infra*).

Moreover, a specific interaction between the additional aromatic ring of the *p*OoBSK surfactant and the aromatic portion of the pyridinium salts, presumably by π -stacking, strictly confines the latter inside the micellar aggregate. This π - π interaction is reflected in the fluorescence maximum position (see Table 1), which is shifted toward higher energies in *p*OoBSK micelles when compared with SDS aggregates (as opposed to the greater effect provided by this latter environment on the absorption spectrum). Hence, the emission maximum serves as an indicator of the less efficient ICT occurring in the excited states of **1** and **2** in the presence of *p*OoBSK micelles, by virtue of the aforementioned π - π interaction. The fluorescence quantum yields, sensible to the combined effect of viscosity and polarity, are indeed enhanced in both kinds of micelles for both compounds (Table 1).

In order to relate the changes in the spectral properties induced by the micelles to an effective inclusion within the micellar aggregate, spectroscopic and fluorimetric titrations were performed starting from aqueous solutions of the compounds and then adding increasing amounts of surfactant to reach a concentration far exceeding its cmc (Figures 2 and

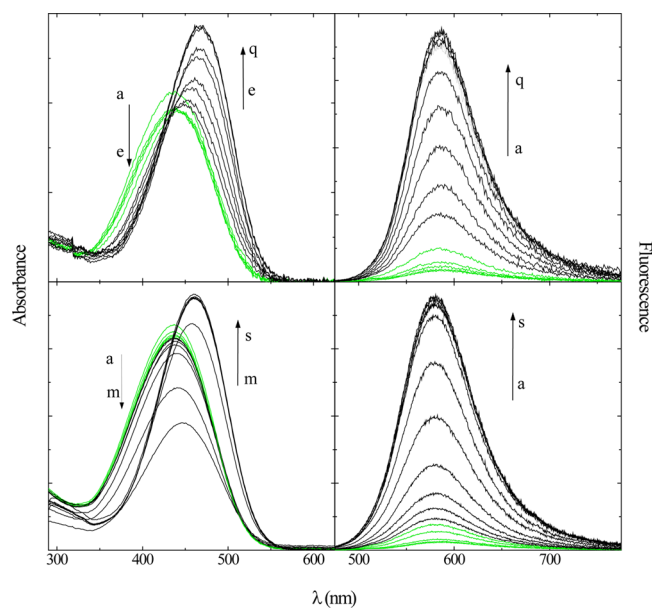


Figure 2. Absorption (left panels) and emission (right panels) spectra of **1** in aqueous solution, alone and in the presence of increasing concentration of the two surfactants (up to 0.03 M): SDS (upper panels, $[1] = 3.1 \times 10^{-6}$ M) and *p*OoBSK (lower panels, $[1] = 3.6 \times 10^{-6}$ M). The spectra recorded before the cmc of SDS and *p*OoBSK are represented as green lines.

Table 1. Spectral Properties and Fluorescence Quantum Yields of Compounds **1** and **2** in DCM, SDS Solution (0.1 M), *p*OoBSK Solution (0.1 M), and W

medium	1				2			
	λ_{abs} (nm)	λ_{em} (nm)	$\Delta\nu$ (cm ⁻¹)	ϕ_{F}	λ_{abs} (nm)	λ_{em} (nm)	$\Delta\nu$ (cm ⁻¹)	ϕ_{F}
DCM ^a	500	590	3090	0.14	393	559	7690	0.012
SDS solution	468	585	4270	0.026	368	535	8480	0.048
<i>p</i> OoBSK solution	460	580	4530	0.027	366	530	8520	0.034
W ^a	438	589	5850	0.001	353	546	10010	0.003

^aData retrieved from ref 36.

3). In the presence of both surfactants, a double trend for all of the compounds is always revealed throughout the titrations, i.e.,

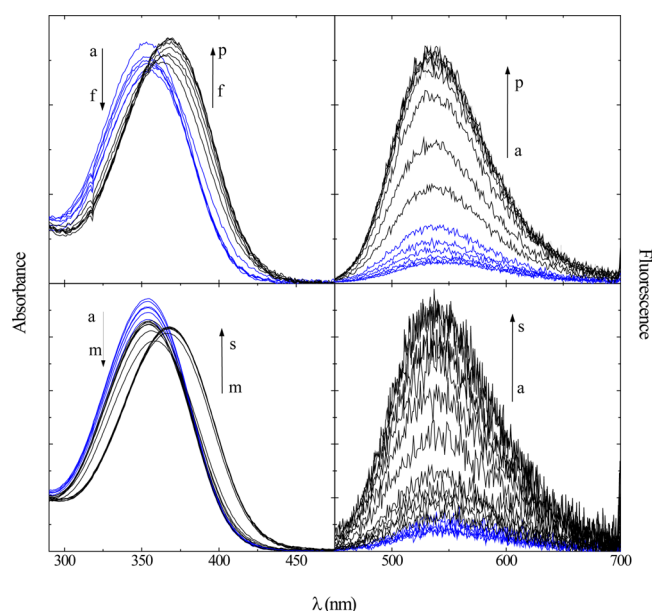


Figure 3. Absorption (left panels) and emission (right panels) spectra of **2** in aqueous solution, alone and in the presence of increasing concentration of the two surfactants (up to 0.03 M): SDS (upper panels, $[2] = 3.4 \times 10^{-6}$ M) and *p*OoBSK (lower panels, $[2] = 4.3 \times 10^{-6}$ M). The spectra recorded before the cmc of SDS and *p*OoBSK are represented as blue lines.

before reaching the cmc and after the formation of some micelles in the solution.

After the first additions of surfactant into the solution, a reduction of the absorption intensity is detected along with a small bathochromic band shift (which is more apparent with *p*OoBSK), while the fluorescence spectrum stays essentially

unchanged (cf. colored spectra in Figures 2 and 3). Beyond the cmc of the two surfactants, major changes are revealed in both absorption and emission properties: the absorption band undergoes a larger *red-shift* and the absorbance increases, while the fluorescence experiences a considerable hyperchromic *blue-shift* (cf. black spectra in Figures 2 and 3). This evidence suggests the occurrence of two distinct events: (1) at low surfactant concentrations, a one-to-one electrostatic interaction between the negatively charged surfactant head and the cationic pyridinium unit, with the resultant formation of a poorly soluble ion pair as indicated by the detection of scattered light at long wavelengths; (2) beyond the cmc, the intercalation of the pyridinium salts inside the micelles, which brings about the *red-shift* of the absorption and the enhancement of the fluorescence emission, as the micelles provide a less polar and more viscous environment.^{54,55}

Femtosecond Transient Absorption Measurements.

Femtosecond transient absorption measurements were carried out on aqueous solutions of the two compounds under investigation in the presence of micelles of SDS and *p*OoBSK. The transient absorption decays were acquired upon excitation with laser pulses centered at 400 nm over a time window of 3200 ps. On the basis of the spectral range of interest for detecting the transient signals of each compound, we resorted to a sapphire and a CaF₂ window to generate the probing light in the case of **1** and **2**, respectively.

The physical properties of the medium have already proven to have a discernible effect on the excited state dynamics of the two compounds, leading to two limiting cases: (a) intramolecular charge transfer (ICT) controlled deactivation and (b) solvent controlled deactivation.³⁶ In case a, the Franck–Condon (FC) state, populated by direct absorption of the excitation light, leads to a relaxed locally excited state (LE), defined by a decreased dipole moment with respect to the highly polar ground state. The LE state then evolves into an ICT state, by back-transferring the positive charge to the methylpyridinium unit, thus increasing the dipole moment of

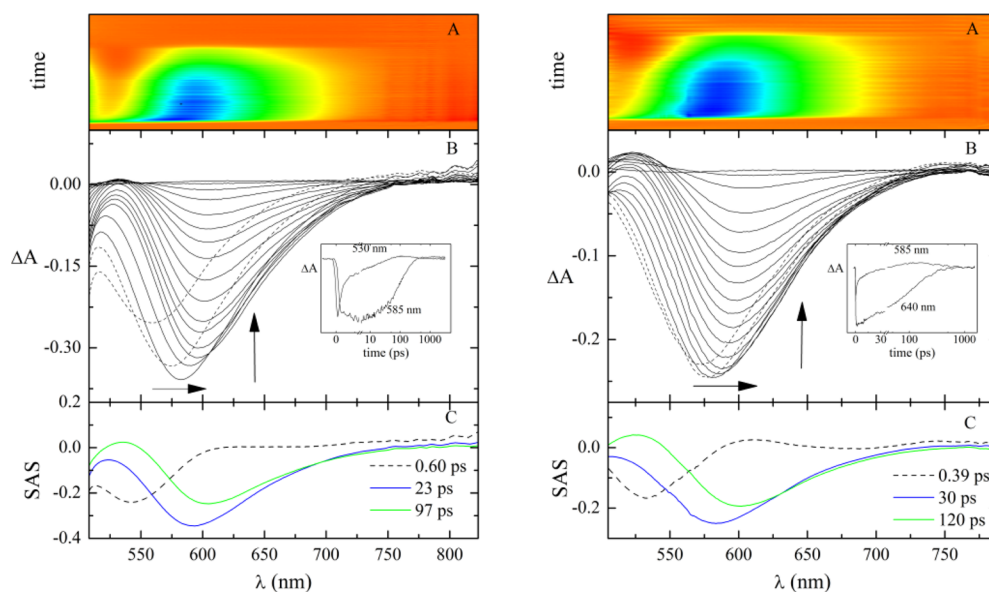


Figure 4. Pump–probe absorption spectroscopy of **1** within SDS (0.1 M) (left graph) and *p*OoBSK (0.1 M) (right graph) solutions ($\lambda_{\text{exc}} = 400$ nm): (A) contour plot of the experimental data, (B) time-resolved absorption spectra (the first two in dashed lines) recorded at increasing delays after the laser pulse (inset: decay kinetics at meaningful wavelengths, with a linear scale for the first picoseconds and a log scale for longer times), and (C) species associated spectra (SAS) calculated by target analysis.

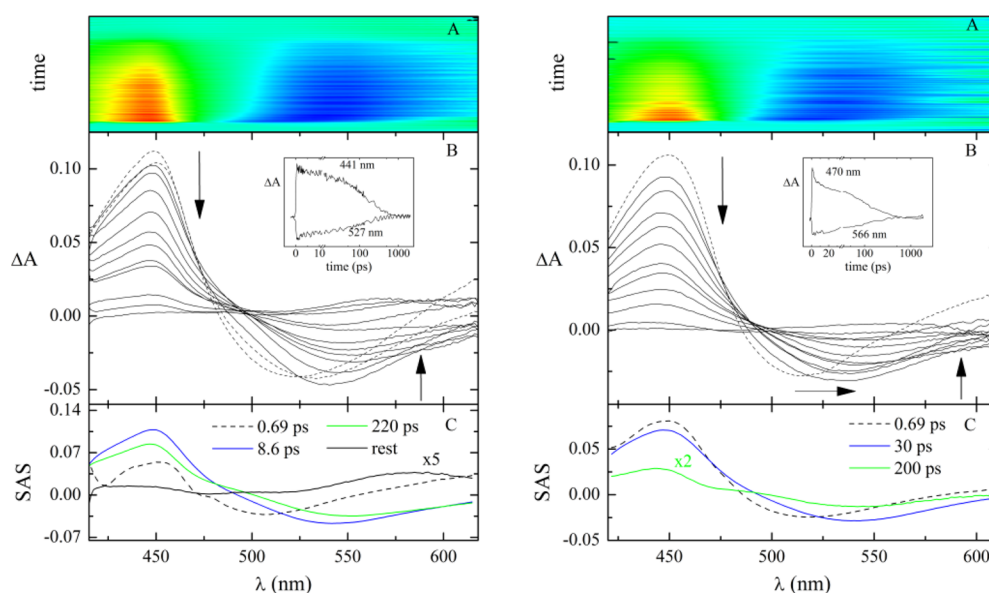


Figure 5. Pump–probe absorption spectroscopy of **2** within SDS (0.1 M) (left graph) and *p*OoBSK (0.1 M) (right graph) solutions ($\lambda_{\text{exc}} = 400$ nm): (A) contour plot of the experimental data, (B) time-resolved absorption spectra (the first ones in dashed lines) recorded at increasing delays after the laser pulse (inset: decay kinetics at meaningful wavelengths, with a linear scale for the first picoseconds and a log scale for longer times), and (C) species associated spectra (SAS) calculated by target analysis.

Table 2. Excited State Spectral and Kinetic Properties of Compounds 1 and 2 in DCM, SDS (0.1 M) Solution, *p*OoBSK (0.1 M) Solution, and W Obtained by Femtosecond Transient Absorption Spectroscopy ($\lambda_{\text{exc}} = 400$ nm)^a

medium	1		2		assignment
	λ (nm)	τ (ps)	λ (nm)	τ (ps)	
DCM ^b	<540(-)	0.70	520(-), 635(+)	0.68	Solv.
	585(-)	52	555(-)	10	¹ LE*
	550(+), 605(-)	134	575(-)	172	¹ ICT*
	580(+)	rest			T ₁
SDS solution	540(-), 615(+)	0.61	450(+), 505(-), >555(+)	0.69	Solv.
	590(-)	23	450(+), 540(-)	8.6	¹ LE*
	535(+), 605(-)	97	445(+), 550(-)	220	¹ ICT*
<i>p</i> OoBSK solution	535(-), 610(+)	0.39	435(+), 585(+)	rest	T ₁
	585(-)	30	450(+), 520(-)	0.69	Solv.
	525(+), 600(-)	120	445(+), 540(-)	30	¹ LE*
W ^b			445(+), 545(-)	200	¹ ICT*
	560(-)	0.70	560(+)	0.24	Solv _i
	520(+), 615(-)	4.4	515(-), 630(+)	0.91	Solv _d / ¹ LE*
			25	¹ ICT*	

^aSpectral properties refer to the species associated spectra (SAS) calculated by target analysis. The symbols (+) and (-) stand for positive and negative signals, respectively. ^bData retrieved from ref 36.

the relaxed excited state. Through quantum-mechanical calculations, the latter was found to be twisted (TICT) in the case of compounds **1** and **2** in polar solvents.³⁶ Hence, in polar environments, the two molecules experience lower energy barriers during the ICT process and lose the net separation between the LE and ICT states. The latter is directly populated along with solvent relaxation (case b). The excited state deactivation scheme of the two molecules is therefore very revealing about the environment they can experience.

Looking at the time-resolved spectra of the compounds (panel B of Figures 4 and 5), large spectral shifts are observed: negative signals of stimulated emission shift to lower energies over time. These substantial evolutions reflect the stabilization of the excited states occurring together with their deactivation: larger shifts mean more energetically stabilized excited states,

that is to say a more efficient intramolecular charge transfer. The spectral evolution of compound **1** (Figure 4) is described by a broad region of negative signal, in correspondence to its stationary fluorescence spectral range, and it is thus assigned to the stimulated emission promoted by the white-light continuum probe. This negative band moves toward lower energies while decaying within hundreds of picoseconds. Compound **2** (Figure 5) shows a significant stimulated emission signal in the 500–600 nm range, red-shifting during the measurements, and a strong transient absorption band at shorter wavelengths; both bands fully decay in less than 1000 ps. Similar spectra were recorded in *p*OoBSK micelles for the two molecules.

The results of target analysis are shown in panel C of the concerning figures and listed in Table 2, together with data

Table 3. Triplet Spectral and Kinetic Properties of **1** and **2** in W, SDS (0.1 M) Solution, and DCM Obtained by Nanosecond-Laser Flash Photolysis ($\lambda_{\text{exc}} = 355 \text{ nm}$)

medium	1				2			
	λ_{max} (nm)	τ_T (μs)	$\phi_T \times \epsilon_T$ ($\text{M}^{-1} \text{cm}^{-1}$)	k_{ox} ($\text{M}^{-1} \text{s}^{-1}$)	λ_{max} (nm)	τ_T (μs)	$\phi_T \times \epsilon_T$ ($\text{M}^{-1} \text{cm}^{-1}$)	k_{ox} ($\text{M}^{-1} \text{s}^{-1}$)
DCM ^a	600	1.6	5130	1.2×10^9	450	5	930	
	860	1.2						
SDS solution	590	100	380	3.1×10^8	440	120	200	1.1×10^8
	740	0.67		8.0×10^9	690	1.6		1.0×10^{10}
W ^a	570	14	250	1.5×10^9	430	125	160	2.2×10^9
	730	0.41		2.9×10^{10}	710	0.47		1.1×10^{10}

^aData retrieved from ref 37.

referring to the same molecules in the polar aqueous solution (W) and in the much less polar DCM.

The global and target analysis pointed out the contribution of three transients to the relaxation dynamics in both micellar media for both compounds: the shortest component (S) is assigned to a fast solvent equilibration, as the one previously seen in both DCM and W (e.g., for compound **1**, $\tau_S = 0.61$ and 0.39 ps in SDS and *p*OoBSK, respectively, and $\tau_S = 0.70 \text{ ps}$ in homogeneous solution). In fact, anionic surfactant micelles are expected to provide the methylpyridinium derivatives with a rather thin hydration layer, keeping them exposed to the solvent to a certain degree.⁵⁶ After the solvation has occurred, in aqueous solution, the deactivation process is reported to be extremely efficient with a time constant of 4.4 ps for **1** and 25 ps for **2**.³⁶ This transient is assigned to a twisted ICT state, populated from the LE state during solvent relaxation (case b). However, in the presence of micelles and just like what has been observed in nonpolar solvents (as reported for DCM),³⁶ two distinct electronic states are detected: an intermediate component assigned to the relaxed LE state and a longer-living component assigned to an ICT state. The detection of these two distinct states offers evidence of the inclusion of the molecule within the micellar aggregate, where the less polar environment is responsible for a net separation between the two states (ICT-controlled deactivation, case a).

The comparison between the two micellar media reveals longer time constants for the intermediate component when the *p*OoBSK is considered ($\tau_{\text{LE}} = 30$ vs 23 ps for compound **1** and $\tau_{\text{LE}} = 30$ vs 8.6 ps for compound **2** in *p*OoBSK and SDS, respectively). These findings can be adequately explained by taking into account the surfactant structures and the aromatic ring of the *p*OoBSK molecule. The π -stacking interaction between the surfactant and the two compounds has been already invoked for the rationalization of the differences in the alterations of the photophysical properties induced by the two kinds of micelles: this interaction supposedly causes the LE lifetime to lengthen by slowing down the back-charge transfer and hindering the twisting which would lead to the fast formation of the ICT state.

Despite the difference in the donor unit of the two compounds, especially reflected in the peculiar fluorescence quantum yields (larger for **2** than **1**) and excited state lifetimes (longer for **2** than **1**) observed in pure aqueous solution, the two pyridinium cations exhibit similar photophysical behavior when dissolved in the same surfactant solution. These interesting results unravel that the nature of the surfactant, defining the microenvironment experienced by the probes, is the key factor in determining their excited state properties.

Flash Photolysis Measurements. Nanosecond-resolved laser flash photolysis measurements were performed on the two

molecules under investigation in the presence of both surfactant micelles. Table 3 shows the results referring to SDS solutions, compared to the data collected in W and in DCM.

The deactivation of the triplet state of the two compounds in the presence of SDS micelles showed a behavior resembling the one previously detected in water,³⁷ although they experience a scarcely polar environment: the transient absorption spectra in micelles and those in aqueous solution are much more similar than those in solvents such as acetonitrile or DCM. The deactivation kinetics is well described by two components with independent decays and different spectral shapes. As shown in Figures 6 and 7 for compounds **1** and **2**, respectively, the

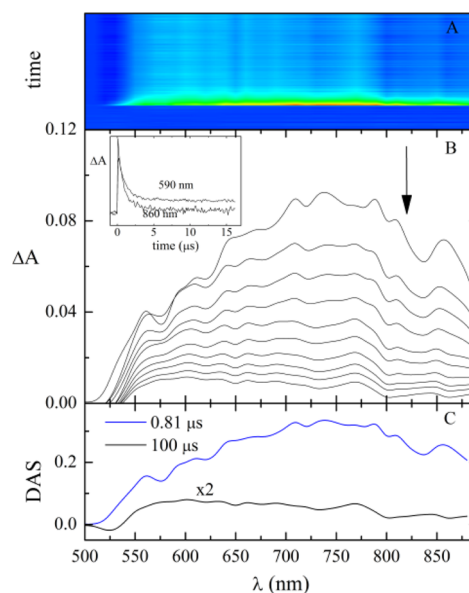


Figure 6. Transient absorption spectroscopy of **1** in SDS (0.1 M) solution ($\lambda_{\text{exc}} = 355 \text{ nm}$): (A) contour plot of the experimental data, (B) time-resolved absorption spectra recorded at increasing delays after the laser pulse (inset: decay kinetics at meaningful wavelengths), and (C) decay associated spectra (DAS) of the decay components obtained by SVD and global analysis.

longer-living component, which absorbs at shorter wavelengths, has been already assigned to the $T_{1 \rightarrow T_n}$ transient absorption, whereas the fast component shows a broad band at lower energies and is associated with the hydrated electron formed by photoinduced ejection from the donor moiety of **1** and **2**.³⁷

In spite of the similarities with the spectral evolutions acquired in water, evidence of the inclusion of the molecules inside the micellar aggregate can still be found: (i) the time

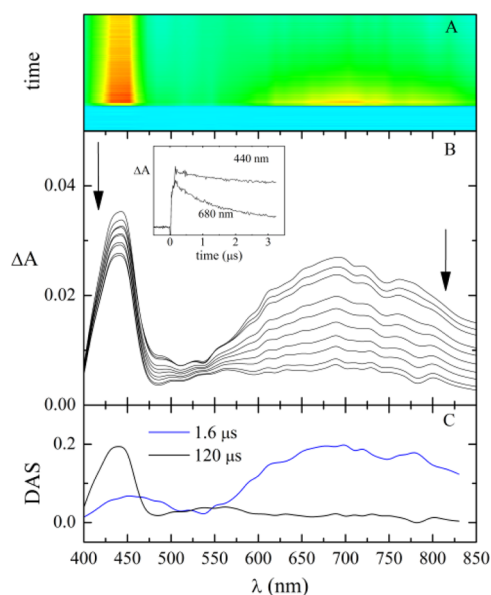


Figure 7. Transient absorption spectroscopy of **2** in SDS (0.1 M) solution ($\lambda_{\text{exc}} = 355$ nm): (A) contour plot of the experimental data, (B) time-resolved absorption spectra recorded at increasing delays after the laser pulse (inset: decay kinetics at meaningful wavelengths), and (C) decay associated spectra (DAS) of the decay components obtained by SVD and global analysis.

constant of the longer-living T_1 transient (hundreds of microseconds) is generally longer than the same component detected in aqueous solution; (ii) its absorption band is slightly red-shifted comparing to the same in pure water; (iii) its formation quantum yield (ϕ_T) increases according to a reduced polarity effect; (iv) it is quenched by molecular oxygen at a slower rate than the diffusional one ($k_{\text{ox}} \sim 10^8 \text{ M}^{-1} \text{ s}^{-1}$). The concentration of oxygen inside a micellar aggregate is indeed expected to be lower than that in the bulk aqueous solution,⁵⁷ and a less efficient oxygen quenching is thus envisaged. On the other hand, the transient associated with the hydrated electron is probably ejected out of the micelle and into the aqueous medium and thus strongly affected by oxygen ($k_{\text{ox}} \sim 10^{10} \text{ M}^{-1} \text{ s}^{-1}$), as it was previously found in the experiments performed in homogeneous aqueous solution.³⁷ However, the lifetime lengthening of this transient is supposedly due to the hindered recombination with the radical species, which might still be placed within the micellar aggregate.

Differently, these compounds in *p*OoBSK micelles proved to be extremely reactive upon laser irradiation and a significant formation of photoproducts was revealed, thus affecting the reliability of the acquired data.

The reason underlying this behavior is provided by the competitive deactivation pathways. The photoisomerization around the central double bond is an operative decay channel for the *trans* isomers of the pyridinium salts, notwithstanding being negligible in solvent of higher polarity. The photoreaction competes with the intramolecular charge transfer, thus becoming a minor deactivation pathway when the efficiency of the ICT state formation and the subsequent internal conversion to the ground state are enhanced (i.e., increasing the solvent polarity or the charge separation). Even the inclusion within the micellar aggregate should induce a less efficient charge transfer, thus fostering both the isomerization in the singlet manifold and the triplet formation, the latter contributing to the isomerization as well.³⁷ Thus, it is not

surprising that the micellar environment causes photoisomerization to occur, especially in the case of *p*OoBSK micelles, where the aforementioned interaction between the phenyl ring of the surfactant and the donor moiety of the *push-pull* compounds might limit the intramolecular charge transfer.

CONCLUSIONS

The effect of the organized medium provided by some anionic micelles on the photophysics of the *trans* isomers of two *push-pull* pyridinium salts was fully characterized through steady-state and time-resolved spectroscopic techniques. By combining all the information gathered from the new experiments performed and the thorough knowledge of these molecules acquired from the literature and previous studies, we gained a deep insight into the nanoheterogeneous environment experienced by the pyridinium salts.

Both molecules were found to be readily solubilized by the anionic micellar aggregates. The electrostatic attraction between the negatively charged surfactant heads and the positively charged pyridinium ring proved to be the driving force behind the prompt interaction leading to an efficient inclusion within the micelles. The low polarity and confining conditions provided by the micellar aggregate are responsible for the distinctive spectral and photophysical properties shown by these molecules. The absorption spectrum undergoes a major *red-shift* and the fluorescence quantum yield is enhanced by at least 1 order of magnitude in the case of both compounds if compared to the pure water solution. A comparison between the two surfactants revealed a reduced efficiency of the intramolecular charge-transfer process operative in the excited state in the case of the aromatic *p*OoBSK with respect to the SDS surfactant, as a consequence of the π,π interaction between the phenyl ring of the surfactant and those of the methylpyridinium salts.

Moreover, the excited-state dynamics in the singlet and triplet manifold are instrumental, since the ICT state deactivation channels and its formation from the locally excited (LE) state or via direct solvent relaxation depend on the polarity and viscosity features of the chemical surroundings. The detection of a transient associated with the LE state and the slowed down deactivation of the ICT singlet state, together with a significant concomitant population of the triplet state, are all indicators of a micellar medium characterized by lower polarity and confining properties.

These two methylpyridinium salts proved therefore to be a telling probe of the local environment. Their inclusion within the anionic micelles could also be exploited for their solubilization and targeted delivery, in order to put to use their potential pharmacological activity.

AUTHOR INFORMATION

Corresponding Author

*E-mail: alex.cesaretti14@gmail.com. Phone: +39 0755855574.

Notes

The authors declare no competing financial interest.

ACKNOWLEDGMENTS

The authors thank MIUR (Ministero dell'Università e della Ricerca, Rome, Italy) and University of Perugia (PRIN 2010–2011, no. 2010FM738P, and FIRB 2013, no. RBFR13PSB6) for funding.

REFERENCES

- (1) Fortuna, C. G.; Barresi, V.; Bonaccorso, C.; Consiglio, G.; Failla, S.; Trovato-Salinaro, A.; Musumarra, G. Design, Synthesis and *In Vitro* Antitumour Activity of New Heteroaryl Ethylenes. *Eur. J. Med. Chem.* **2012**, *47*, 221–227.
- (2) Bradamante, S.; Facchetti, A.; Pagani, G. A. Heterocycles As Donor and Acceptor Units in Push–Pull Conjugated Molecules. Part I. *J. Phys. Org. Chem.* **1997**, *10*, 514–524.
- (3) Ephardt, H.; Fromherz, P. Fluorescence and Photoisomerization of an Amphiphilic Aminostilbazolium Dye As Controlled by the Sensitivity of Radiationless Deactivation to Polarity and Viscosity. *J. Phys. Chem.* **1989**, *93*, 7717–7725.
- (4) Fromherz, P.; Heilemann, A. Twisted Internal Charge Transfer in (Aminophenyl) Pyridinium. *J. Phys. Chem.* **1992**, *96*, 6864–6866.
- (5) Gawinecki, R.; Trzebiatowska, K. The Effect of the Amino Group on the Spectral Properties of Substituted Styrylpyridinium Salts. *Dyes Pigm.* **2000**, *45*, 103–107.
- (6) Carlotti, B.; Spalletti, A.; Šindler-Kulyk, M.; Elisei, F. Ultrafast Photoinduced Intramolecular Charge Transfer in Push–Pull Distyryl Furan and Benzofuran: Solvent and Molecular Structure Effect. *Phys. Chem. Chem. Phys.* **2011**, *13*, 4519–4528.
- (7) Flamini, R.; Tomasi, M.; Marrocchi, A.; Carlotti, B.; Spalletti, A. Synthesis and Photobehaviour of Donor- π -Acceptor Conjugated Arylacetylenes. *J. Photochem. Photobiol., A* **2011**, *223*, 140–148.
- (8) Carlotti, B.; Flamini, R.; Spalletti, A.; Marrocchi, A.; Elisei, F. Comprehensive Photophysical Behaviour of Ethynyl Fluorenes and Ethynyl Anthracenes Investigated by Fast and Ultrafast Time-Resolved Spectroscopy. *ChemPhysChem* **2012**, *13*, 724–735.
- (9) Kikaš, I.; Carlotti, B.; Škorić, I.; Šindler-Kulyk, M.; Mazzucato, U.; Spalletti, A. Synthesis, Spectral Properties and Photobehaviour of Push–Pull Distyrylbenzene Nitro-Derivatives. *J. Photochem. Photobiol., A* **2012**, *244*, 38–46.
- (10) Carlotti, B.; Kikaš, I.; Škorić, I.; Spalletti, A.; Elisei, F. Photophysics of Push–Pull Distyrylfurans, Thiophenes and Pyridines by Fast and Ultrafast Techniques. *ChemPhysChem* **2013**, *14*, 970–981.
- (11) Carlotti, B.; Benassi, E.; Barone, V.; Consiglio, G.; Elisei, F.; Mazzoli, A.; Spalletti, A. Effect of π -Bridge and the Acceptor on the Intramolecular Charge Transfer in Push–Pull Cationic Chromophores: a Joint Ultrafast Spectroscopic and TD-DFT Computational Study. *ChemPhysChem* **2015**, DOI: 10.1002/cphc.201402896.
- (12) Carlotti, B.; Cesaretti, A.; Fortuna, C. G.; Spalletti, A.; Elisei, F. Experimental Evidence of Dual Emission in a Negatively Solvatochromic Push–Pull Pyridinium Derivative. *Phys. Chem. Chem. Phys.* **2014**, *17*, 1877–1882.
- (13) Carlotti, B.; Benassi, E.; Spalletti, A.; Fortuna, C. G.; Elisei, F.; Barone, V. Photoinduced Symmetry-Breaking Intramolecular Charge Transfer in a Quadrupolar Pyridinium Derivative. *Phys. Chem. Chem. Phys.* **2014**, *16*, 13984–13994.
- (14) Benassi, E.; Carlotti, B.; Fortuna, C. G.; Barone, V.; Elisei, F.; Spalletti, A. Acid–Base Strength and Acidochromism of Some Dimethylamino–Azinium Iodides. An Integrated Experimental and Theoretical Study. *J. Phys. Chem. A* **2015**, *119*, 323–333.
- (15) Fortuna, C. G.; Bonaccorso, C.; Qamar, F.; Anu, A.; Ledoux, I.; Musumarra, G. Synthesis and NLO Properties of New Trans 2-(Thiophen-2-yl) Vinyl Heteroaromatic Iodides. *Org. Biomol. Chem.* **2011**, *9*, 1608–1613.
- (16) Fortuna, C. G.; Forte, G.; Pittalà, V.; Giuffrida, A.; Consiglio, G. Could 2, 6-Bis ((E)-2-(Furan-2-yl) Vinyl)-1-Methylpyridinium Iodide and Analog Compounds Intercalate DNA? A First Principle Prediction Based on Structural and Electronic Properties. *Comput. Theor. Chem.* **2012**, *985*, 8–13.
- (17) Mazzoli, A.; Carlotti, B.; Fortuna, C. G.; Spalletti, A. Photobehaviour and DNA Interaction of Styrylquinolinium Salts Bearing Thiophene Substituents. *Photochem. Photobiol. Sci.* **2011**, *10*, 973–979.
- (18) Mazzoli, A.; Carlotti, B.; Bonaccorso, C.; Fortuna, C. G.; Mazzucato, U.; Miolo, G.; Spalletti, A. Photochemistry and DNA-Affinity of Some Pyrimidine-Substituted Styryl-Azinium Iodides. *Photochem. Photobiol. Sci.* **2011**, *10*, 1830–1836.
- (19) Mazzoli, A.; Carlotti, B.; Consiglio, G.; Fortuna, C. G.; Miolo, G.; Spalletti, A. Photobehaviour of Methyl-Pyridinium and Quinolinium Iodide Derivatives, Free and Complexed with DNA. A Case of Bisintercalation. *Photochem. Photobiol. Sci.* **2014**, *13*, 939–950.
- (20) Fortuna, C. G.; Mazzucato, U.; Musumarra, G.; Pannacci, D.; Spalletti, A. Photochemistry and DNA-Affinity of Some Stilbene and Distyrylbenzene Analogues Containing Pyridinium and Imidazolium Iodides. *J. Photochem. Photobiol., A* **2010**, *216*, 66–72.
- (21) Marri, E.; Mazzucato, U.; Fortuna, C. G.; Musumarra, G.; Spalletti, A. Photobehaviour of Some 1-Heteroaryl-2-(1-Methylpyridinium-2-yl) Ethene Iodides (Free and Complexed with DNA). *J. Photochem. Photobiol., A* **2006**, *179*, 314–319.
- (22) Torchilin, V. P. Micellar Nanocarriers: Pharmaceutical Perspectives. *Pharm. Res.* **2007**, *24*, 1–16.
- (23) Rangel-Yagui, C. O.; Pessoa, A., Jr; Tavares, L. C. Micellar Solubilization of Drugs. *J. Pharm. Pharm. Sci.* **2005**, *8*, 147–163.
- (24) Mazzoli, A.; Spalletti, A.; Carlotti, B.; Emiliani, C.; Fortuna, C. G.; Urbanelli, L.; Tarpani, L.; Germani, R. Spectroscopic Investigation of Interactions of New Potential Anticancer Drugs with DNA and Non-Ionic Micelles. *J. Phys. Chem. B* **2015**, *119*, 1483–1495.
- (25) Enache, M.; Anghelache, I.; Volanschi, E. Coupled Spectral and Electrochemical Evaluation of the Anticancer Drug Mitoxantrone–Sodium Dodecyl Sulfate Interaction. *Int. J. Pharm.* **2010**, *390*, 100–106.
- (26) Enache, M.; Volanschi, E. Spectral Studies on the Molecular Interaction of Anticancer Drug Mitoxantrone with CTAB Micelles. *J. Pharm. Sci.* **2011**, *100*, 558–565.
- (27) Enache, M.; Volanschi, E. Spectroscopic Investigations of the Molecular Interaction of Anticancer Drug Mitoxantrone with Non-Ionic Surfactant Micelles. *J. Pharm. Pharmacol.* **2012**, *64*, 688–696.
- (28) Sahoo, D.; Chakravorti, S. Spectra and Dynamics of an Ionic Styryl Dye in Reverse Micelles. *J. Photochem. Photobiol., A* **2009**, *205*, 129–138.
- (29) Schreier, S.; Malheiros, S. V.; de Paula, E. Surface Active Drugs: Self-Association and Interaction with Membranes and Surfactants. Physicochemical and Biological Aspects. *Biochim. Biophys. Acta, Biomembr.* **2000**, *1508*, 210–234.
- (30) Cesaretti, A.; Carlotti, B.; Gentili, P. L.; Clementi, C.; Germani, R.; Elisei, F. Spectroscopic Investigation of the pH Controlled Inclusion of Doxycycline and Oxytetracycline Antibiotics in Cationic Micelles and Their Magnesium Driven Release. *J. Phys. Chem. B* **2014**, *118*, 8601–8613.
- (31) Wandelt, B.; Turkewitsch, P.; Stranix, B. R.; Darling, G. D. Effect of Temperature and Viscosity on Intramolecular Charge-Transfer Fluorescence of a 4-*p*-Dimethylaminostyrylpyridinium Salt in Protic Solvents. *J. Chem. Soc., Faraday Trans.* **1995**, *91*, 4199–4205.
- (32) Ramadass, R.; Bereiter-Hahn, J. How DASPMI Reveals Mitochondrial Membrane Potential: Fluorescence Decay Kinetics and Steady-State Anisotropy in Living Cells. *Biophys. J.* **2008**, *95*, 4068–4076.
- (33) Ramadass, R.; Bereiter-Hahn, J. Photophysical Properties of DASPMI as Revealed by Spectrally Resolved Fluorescence Decays. *J. Phys. Chem. B* **2007**, *111*, 7681–7690.
- (34) Sahoo, D.; Bhattacharya, P.; Chakravorti, S. On the Spectral Behavior of an Ionic Styryl Dye: Effect of Micelle–Polyethylene-block-polyethylene Glycol Diblock Copolymer Assembly. *J. Phys. Chem. B* **2009**, *113*, 13560–13565.
- (35) Letrun, R.; Koch, M.; Dekhtyar, M. L.; Kurdyukov, V. V.; Tolmachev, A. I.; Rettig, W.; Vauthey, E. Ultrafast Excited-State Dynamics of Donor–Acceptor Biaryls: Comparison between Pyridinium and Pyrilyum Phenolates. *J. Phys. Chem. A* **2013**, *117*, 13112–13126.
- (36) Carlotti, B.; Consiglio, G.; Elisei, F.; Fortuna, C. G.; Mazzucato, U.; Spalletti, A. Intramolecular Charge Transfer of Push–Pull Pyridinium Salts in the Singlet Manifold. *J. Phys. Chem. A* **2014**, *118*, 3580–3592.
- (37) Carlotti, B.; Consiglio, G.; Elisei, F.; Fortuna, C. G.; Mazzucato, U.; Spalletti, A. Intramolecular Charge Transfer of Push–Pull

Pyridinium Salts in the Triplet Manifold. *J. Phys. Chem. A* **2014**, *118*, 7782–7787.

(38) Strehmel, B.; Seifert, H.; Rettig, W. Photophysical Properties of Fluorescence Probes. 2. A Model of Multiple Fluorescence for Stilbazolium Dyes Studied by Global Analysis and Quantum Chemical Calculations. *J. Phys. Chem. B* **1997**, *101*, 2232–2243.

(39) Bales, B. L.; Messina, L.; Vidal, A.; Peric, M.; Nascimento, O. R. Precision Relative Aggregation Number Determinations of SDS Micelles Using a Spin Probe. A Model of Micelle Surface Hydration. *J. Phys. Chem. B* **1998**, *102*, 10347–10358.

(40) Bunton, C. A.; Romsted, L. S.; Savelli, G. Tests of the Pseudophase Model of Micellar Catalysis: Its Partial Failure. *J. Am. Chem. Soc.* **1979**, *101*, 1253–1259.

(41) Liu, Y.-L.; Liu, L.; Wang, Y.-L.; Han, Y.-C.; Wang, D.; Chen, Y.-J. Calix[n]arene Sulfonic Acids Bearing Pendant Aliphatic Chains as Recyclable Surfactant-Type Brønsted Acid Catalysts for Allylic Alkylation with Allyl Alcohols in Water. *Green Chem.* **2008**, *10*, 635–640.

(42) Butschies, M.; Frey, W.; Laschat, S. Designer Ionic Liquid Crystals Based on Congruently Shaped Guanidinium Sulfonates. *Chem.—Eur. J.* **2012**, *18*, 3014–3022.

(43) Bartocci, G.; Masetti, F.; Mazzucato, U.; Spalletti, A.; Baraldi, I.; Momicchioli, F. Photophysical and Theoretical Studies of Photoisomerism and Rotamerism of Trans-Styrylphenanthrenes. *J. Phys. Chem.* **1987**, *91*, 4733–4743.

(44) Cesaretti, A.; Carlotti, B.; Clementi, C.; Germani, R.; Elisei, F. Effect of Micellar and Sol–Gel Media on the Spectral and Kinetic Properties of Tetracycline and Its Complexes with Mg²⁺. *Photochem. Photobiol. Sci.* **2014**, *13*, 509–520.

(45) Carlotti, B.; Cesaretti, A.; Elisei, F. Complexes of Tetracyclines with Divalent Metal Cations Investigated by Stationary and Femto-second-Pulsed Techniques. *Phys. Chem. Chem. Phys.* **2012**, *14*, 823–834.

(46) Cesaretti, A.; Carlotti, B.; Gentili, P. L.; Clementi, C.; Germani, R.; Elisei, F. Doxycycline and Oxytetracycline Loading of a Zwitterionic Amphoteric Surfactant-Gel and Their Controlled Release. *Phys. Chem. Chem. Phys.* **2014**, *16*, 23096–23107.

(47) Golub, G. H.; Loan, C. F. V. *Matrix Computations*; The John Hopkins University Press: Baltimore, MD, 1996.

(48) Strang, G. *Introduction to Linear Algebra*; Wellesley-Cambridge Press: Wellesley, MA, 1998.

(49) Snellenburg, J.; Laptinok, S.; Seger, R.; Mullen, K.; Van Stokkum, I. Glotaran: A Java-Based Graphical User Interface for the R Package TIMP. *J. Stat. Software* **2012**, *49*, 1.

(50) van Stokkum, I. H.; Larsen, D. S.; van Grondelle, R. Global and Target Analysis of Time-Resolved Spectra. *Biochim. Biophys. Acta, Bioenerg.* **2004**, *1657*, 82–104.

(51) Görner, H.; Elisei, F.; Aloisi, G. G. Photoinduced Electron Transfer Between Styrylanthracenes and Electron Donors and Acceptors in Acetonitrile. *J. Chem. Soc., Faraday Trans.* **1992**, *88*, 29–34.

(52) Romani, A.; Elisei, F.; Masetti, F.; Favaro, G. pH-Induced Effects on the Photophysics of Dipyrindyl Ketones. *J. Chem. Soc., Faraday Trans.* **1992**, *88*, 2147–2154.

(53) Carmichael, I.; Hug, G. L. Triplet–Triplet Absorption Spectra of Organic Molecules in Condensed Phases. *J. Phys. Chem. Ref. Data* **1986**, *15*, 1–250.

(54) Ghatak, C.; Rao, V. G.; Mandal, S.; Ghosh, S.; Sarkar, N. An Understanding of the Modulation of Photophysical Properties of Curcumin Inside a Micelle Formed by an Ionic Liquid: a New Possibility of Tunable Drug Delivery System. *J. Phys. Chem. B* **2012**, *116*, 3369–3379.

(55) Sanz-Medel, A.; de La Campa, R. F.; Alonso, J. I. G. Metal Chelate Fluorescence Enhancement in Micellar Media: Mechanisms of Surfactant Action. *Analyst* **1987**, *112*, 493–497.

(56) Bhattacharyya, K. Solvation Dynamics and Proton Transfer in Supramolecular Assemblies. *Acc. Chem. Res.* **2003**, *36*, 95–101.

(57) Step, E. N.; Turro, N. J. Photolysis of Ketones in Oxygen-Saturated Micellar Solution: Oxygen Scavenging of C-Centered

Radicals in Microheterogeneous Media. *J. Photochem. Photobiol., A* **1994**, *84*, 249–256.